Earthquakes and Structures, *Vol. 14, No. 3 (2018) 187-201*
DOI: https://doi.org/10.12989/eas.2018.14.3.187

Modified cyclic steel law including bond-slip for analysis of RC structures with plain bars

Silvia Caprili[1], Francesca Mattei[*2], Rosario Gigliotti[2] and Walter Salvatore[1]

[1]*Department of Civil and Industrial Engineering, University of Pisa, 1 Largo L. Lazzarino, 56126, Pisa, Italy*
[2]*Department of Structural and Geotechnical Engineering, University of Rome La Sapienza, 18 Eudossiana St., 00184, Rome, Italy*

(Received November 23, 2017, Revised January 29, 2018, Accepted February 4, 2018)

Abstract. The paper describes a modified cyclic bar model including bond-slip phenomena between steel reinforcing bars and surrounding concrete. The model is focused on plain bar and is useful, for its simplicity, for the seismic analyses of RC structures with plain bars and insufficient constructive details, such as in the case of '60s -'70s Mediterranean buildings. The model is based on an imposed exponential displacements field along the bar including both steel deformation and slip; through the adoption of equilibrium and compatibility equations a stress-slip law can be deducted and simply applied, with opportune operations, to RC numerical models. This study aims to update and complete the original monotonic model published by the authors, solving some numerical inconsistencies and, mostly, introducing the cyclic formulation. The first aim is achieved replacing the imposed linear displacement field along the bar with an exponential too, while the cyclic behaviour is described through a formulation based on the results of parametric analyses concerning a large range of steel and concrete properties and geometric configurations. Validations of the proposed model with experimental results available in the current literature confirm its accuracy and the reduced computational burden, highlighting its suitability in performing nonlinear analyses of RC structures.

Keywords: bond slip; plain bars; existing structures; fiber elements; cyclic/seismic behavior

1. Introduction

The modelling of bond slip phenomena between steel bars and surrounding concrete represents a relevant issue in the description of the cyclic response of Reinforced Concrete (RC) sections, elements and whole structures, especially in the case of existing buildings where plain bars are used, often in conjunction with poor anchorage conditions and insufficient lap spliced. The inadequacy of structural detailing and the following degradation of bond strength cause an insufficient available ductility in presence of cyclic loads: as highlighted by a lot of past and recent experimental investigations (Filippou *et al*. 1983, Hakuto *et al*. 2000, Gigliotti *et al*. 2002, Varum *et al*. 2015, Fernandes *et al*. 2013, Mohammad *et al*. 2014, Laterza *et al.* (2017), Morelli *et al.* 2017) a progressive reduction of the strength and of the stiffness of RC elements, mainly in correspondence of those areas where plasticity occurs and cracks open, was observed.

From what above presented, the need of reliable numerical models including relative slip to correctly represent the structural performance of RC structures becomes evident. Several models including bond-slip phenomena where proposed from the 60's to nowadays, mainly divided in continuum and frame models, differing for accuracy and computational time requiring.

Continuum models for bond slip (e.g., Kwak and Filippou 1995, Lowes 1999) provided a very detailed solution requiring, at same time, an excessive computational burden to be applied to a whole multi-storey RC structure. The adoption of frame elements, on the contrary, allowed to describe the global response of RC structures through reasonable computational effort, taking into account plastic phenomena using two different possible approaches: lumped and distributed plasticity.

In the case of lumped plasticity, bond-slip phenomena can be included through nonlinear rotational springs located at the end of RC elements (Lowes and Altoontash 2003, Mitra and Lowes 2007, Sezen and Setzler 2008): this modeling approach introduces a discontinuity in the element, needing consequently to define the rotational spring relationship. Among distributed plasticity approach, Monti *et al*. (1997, 2000) proposed to replace the steel fiber with the 'pull-out' fiber representing the slip phenomenon. All these models, however, even though more rigorous and complete, require a very high computational burden often connected to numerical convergence problems, limiting their adoption to the case of individual structural elements rather than of the whole structure.

In recent years several simplified approaches, mainly consisting in the adoption of modified stress-strain steel relationships based on reasonable assumptions (Braga *et al.* 2012, Braga *et al.* 2015, Dehestani *et al.* 2015) were proposed for the description of the monotonic behaviour of reinforcing steel bars in RC structures directly including relative slip.

The slip model proposed by Braga *et al*. (2012) and validated through the experimental tests presented by D'Amato *et al*. (2012) allowed the correct representation of

*Corresponding author, Ph.D.
E-mail: francesca.mattei@uniroma1.it

Copyright © 2018 Techno-Press, Ltd.
http://www.techno-press.com/journals/eas&subpage=7
ISSN: 2092-7614 (Print), 2092-7622 (Online)

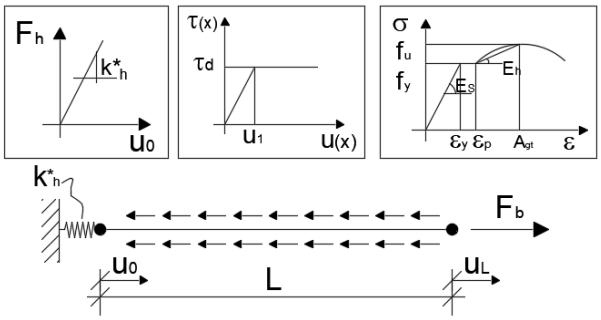

Fig. 1 Scheme of bond-slip model

the behaviour of existing RC elements with plain bars. An extension of this work was later provided by Braga *et al.* (2015) allowing the description of the behaviour of steel bars in the post-elastic field and the determination of the level of deformation imposed by seismic action in buildings designed according to modern standards (Braconi *et al.* 2014). The possibility to evaluate the strain level due to earthquake events on reinforcing steel bars was needed to analyze the effects of corrosion on the ductile performance of traditional steel grades (Caprili and Salvatore 2015, Caprili *et al.* 2015, Salvatore *et al.* 2014).

The present work has the purpose to upgrade the models previously proposed, improving and solving the encountered analytical inconsistencies and, mostly, implementing the cyclic formulation, originally described by a Takeda model based only on empirical considerations. This formulation will allow a larger application of the model in the field of seismic analyses. The simplicity of the proposed model permits investigating the influence of several parameters (i.e., concrete strength, length/diameter ratio, max bond strength and corresponding slip, mechanical properties of steel) on the cyclic steel behaviour and determining bond/slip histories along the bar affected by such problems.

2. Background

The background model (Braga *et al.* 2012, Braga *et al.* 2015) describes the slip field along a hooked end bar of diameter d_b embedded in a concrete block over a certain length (equal to L-total length of the specimen or even lower) under an increasing monotonic displacement u_L applied in correspondence of the free end (Fig. 1) and representing the opening crack at the end element.

The analytical formulation of the model is based on the following assumptions:

- The ***slip field*** along the bar - before yielding - is described by an imposed linear law (Eq. (1)), being u_0 and u_L the end displacements, x the abscissa and L the length of the bar

$$u(x) = u_0 + \frac{(u_0 - u_L)}{L} \cdot x \tag{1}$$

After yielding, the increase of stress due to hardening leads to the increase of relative slip. The development of slip along the bar is then approximated by two different linear branches (Eq. (2)); the parameter L_y, representing the part of the bar in which $u(x) \leq u_y$, being u_y the value of displacement corresponding to the yielding strength, is introduced. If the stress increases, L_y increases too.

$$u(x) = \begin{cases} u_0 + \dfrac{u_y - u_0}{L - L_y} \cdot x & \text{for } 0 \leq x \leq L - L_y \\ u_y + \dfrac{u_L - u_y}{L_y} \cdot (x - L + L_y) & \text{for } L - L_y < x \leq L \end{cases} \tag{2}$$

- The ***bond stress-slip law*** is given by Eq. (3), where τ_d represents the residual bond strength and u_1 is the corresponding slip.

$$\tau[u(x)] = \begin{cases} \dfrac{\tau_d}{u_1} \cdot u(x) & \text{if } u(x) \leq u_1 \\ \tau_d & \text{if } u(x) > u_1 \end{cases} \tag{3}$$

- Any ***anchorage at bar*** end (hook but also bend) can be described by a linear function of the displacement u_0 close to the hook, according to Eq. (4), being F_h is the force acting in correspondence of the anchored end of the bar.

$$F_h = k_h \cdot u_0 \tag{4}$$

- The ***constitutive steel law*** is elastic-perfectly plastic (Braga *et al.* 2012) or elastic-plastic with hardening (Braga *et al.* 2015).

The adoption of equilibrium, compatibility and constitutive equations allows to define the stress and slip fields along the specimen. The equilibrium is given by Eq. (5), where A_b and d_b are, respectively, the cross section and the diameter of the bar.

$$\sigma(x) = \frac{F(x)}{A_b} = \frac{1}{A_b} \cdot \left[\int_0^x \tau(x) \cdot \pi \cdot d_b \cdot dx + F_h \right] = \frac{4}{d_b} \cdot \int_0^x \tau(x) \cdot dx + \frac{F_h}{A_b} \tag{5}$$

The compatibility equation leads to the deduced slip field, Eq. (6)

$$u(x) = u_0 + u_E(x) \tag{6}$$

where the slip along the bar is described in Eq. (7) until the yielding of the bar was reached.

$$u_E(x) = \int_0^x \frac{\sigma(x)}{E_s} dx \tag{7}$$

The stress- slip law at the end of the embedded bar (σ_L-u_L), where the crack opening occurs, can be then derived.

The linearization of the slip field is the most significant simplification in the analytical formulation of the model: D'Amato *et al.* (2012) highlighted relatively small differences comparing the linear schematization of the slip field to other refined formulations (Monti *et al.* 2000), in terms of u_L along the abscissa x. Besides, as visible from Eq. (8)-relative to the case $u_L \leq u_1$, $u_0 \leq u_1$ (Braga *et al.* 2015) - the slip model was affected, in its analytical formulation, by numerical inconsistencies leading to the violation of the compatibility equation: the cubic trend of the slip field can be observed.

$$u(x) = u_0 + \frac{1}{E_S} \cdot \left\{ (k_h^* \cdot u_0) \cdot x + \left(\frac{2 \cdot \tau_d \cdot u_0}{d_b \cdot u_1} \right) \cdot x^2 + \left[\frac{2 \cdot \tau_d}{3 \cdot d_b \cdot u_1 \cdot L} \cdot (u_L - u_0) \right] \cdot x^3 \right\} \tag{8}$$

CASE 1	$u_L \le u_1$, $u_0 < u_1$	***CASE 2***	$u_L > u_1$, $u_0 < u_1$	***CASE 3***	$u_L > u_1$, $u_0 > u_1$
Describes the solution when the value of bond stress is lower than τ_d at both ends of the bar.		Describes the solution when u_L is greater than u_1 (i.e., the bond stress at the free end is equal to τ_d), but u_0 is less than u_1.		Describes the solution when the value of τ_d is reached in the whole bar.	
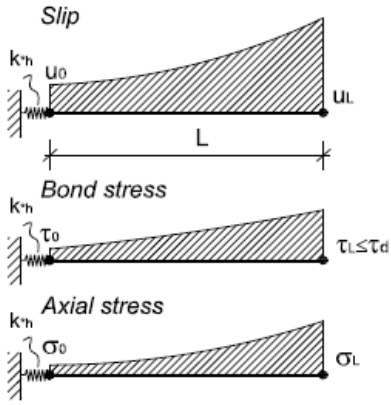		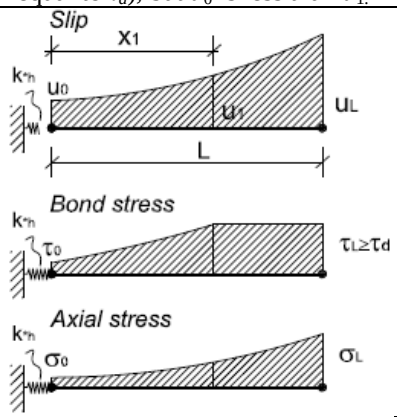		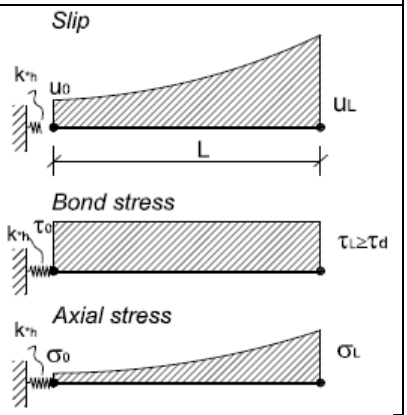	
$\sigma_L = u_0 \cdot \left[\frac{\alpha}{\ln(\gamma_L)} \cdot \frac{E_s}{L} \cdot (\gamma_L - 1) + k_h^* \right]$ (13) $u_L = u_0 \cdot \left\{ 1 + \left\{ \frac{\alpha}{\ln(\gamma_L)} \left[\frac{(\gamma_L - 1)}{\ln(\gamma_L)} - 1 \right] + \beta \right\} \right\}$ (14) $\alpha = \frac{4\tau_d L^2}{E_S \cdot d_b \cdot u_1}$ $\beta = \frac{k_h^* \cdot L}{E_S}$ $\gamma_L = \frac{u_L}{u_0}$ (15)		$\sigma_L = u_0 \cdot \left[\frac{\left(\gamma_L^{\frac{x_1}{L}} - 1 \right)}{L \cdot \ln(\gamma_L)} + \frac{4 \cdot \tau_d \cdot (L - x_1)}{d_b} + k_h^* \right]$ (16) $u_L = u_0 \cdot \left\{ 1 + \left\{ \frac{\alpha}{\ln(\gamma_L)} \cdot \xi + \beta \right\} \right\} + \frac{\alpha \cdot u_1 \ln^2(\gamma_{L1})}{2 \ln^2(\gamma_L)}$ (17) $x_1 = \frac{\ln(\gamma_1)}{\ln(\gamma_L)} \cdot L$ $\gamma_1 = \frac{u_1}{u_0}$ $\xi = \left[\frac{1}{\ln(\gamma_L)} \left(\gamma_L^{\frac{\ln(\gamma_1)}{\ln(\gamma_L)}} - 1 - \ln(\gamma_1) \cdot (\gamma_L)^{\frac{\ln(\gamma_1)}{\ln(\gamma_L)}} \right) + \left(\gamma_L^{\frac{\ln(\gamma_1)}{\ln(\gamma_L)}} - 1 \right) \right]$ (18)		$\sigma_L = k_h^* u_0 + \frac{4 \cdot \tau_d \cdot L}{d_b}$ (19) $u_L = u_0 + \frac{L}{E_S} \left[\frac{2}{d_b} \tau_d L + k_h^* u_0 \right]$ (20)	

Fig. 2 Analytical solution before yielding

Being $k_h^* = \frac{k_h}{A_b}$.

3. The exponential model: analytical formulation of the monotonic behaviour

In the proposed model, the exponential slip field formulation along the bar replaces the linear assumption on which the original slip/hardening models relies. Keeping constant the adoptions concerning the bond stress-slip law (elastic-perfectly plastic) and the anchorage modelling (linear function of u_0), the model is based on the assumptions summarized in Fig. 1:

- The ***slip field*** along the bar is described by an exponential formulation, Eq. (9), in which the symbols have the same meaning as before

$$u(x) = u_0 \cdot \left(\frac{u_L}{u_0} \right)^{\frac{x}{L}} \tag{9}$$

- The ***constitutive law*** for steel is elastoplastic with hardening and plateau.

In this case too, equilibrium, compatibility and constitutive equations shall be used to provide the analytical solution to the problem of a steel bar embedded in a concrete block affected by relative slip. Eq. (5) gives the equilibrium, while the compatibility equations (Eqs. (10)-(11)) provide relative slip before and after the achievement of the yielding stress

$$\Delta u(x) = u_L - u_0 = \int_0^L \frac{\sigma(x)}{E_s} dx = u_E(L) \qquad \sigma(x) \le f_y \tag{10}$$

$$\Delta u(x) = u_L - u_0 = \int_0^{L-L_y} \frac{\sigma(x)}{E_s} dx + \int_{L-L_y}^{L} \varepsilon_p + \frac{\sigma(x) - f_y}{E_h} dx \qquad \sigma(x) > f_y \tag{11}$$

being E_s the elastic modulus of steel and E_h the hardening stiffness of steel, expressed according to Eq. (12), where f_u and f_y are respectively the tensile and yielding strength of

Analytical solution after yielding							
CASE 4	$\sigma_L > f_y,\ u_L \le u_1$	***CASE 5***	$\sigma_L > f_y,\ u_L > u_1,\ u_0 < u_1,\ u_y > u_1$	***CASE 6***	$\sigma_L > f_y,\ u_y < u_1 \le u_L$	***CASE 7***	$\sigma_L > f_y,\ u_L > u_1, u_0 \ge u_1, u_y > u_1$
Condition in which u_L is lower than u_1: the bond stress at the free end is lower than τ_d. The compatibility and equilibrium equations allow the determination of the slip and the stress at the end of the bar (21),(22), being u_y the slip corresponding to the yield stress f_y and L the bar length.		In this case, the slip in correspondence of the free end is higher that u_1 while the bond stress at the hooked end is lower than τ_d.		Condition in which only a portion of the bar is interested by residual friction bond; being x_1 and L_y expressed by (29) and (30), the slip and the stress at the end of the bar are given by (28) and (31)		The bond stress along the bar has a constant value. The expressions of the slip and the stress at the free end are given by:	
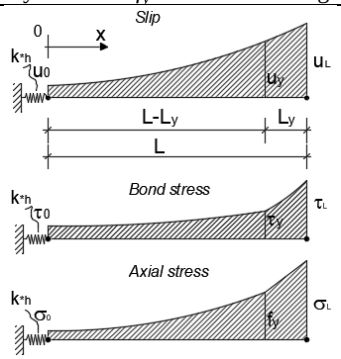		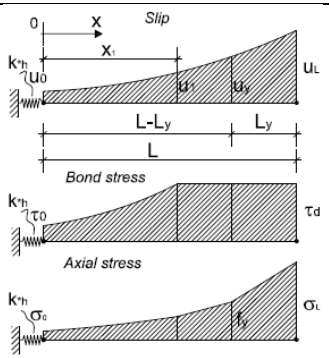		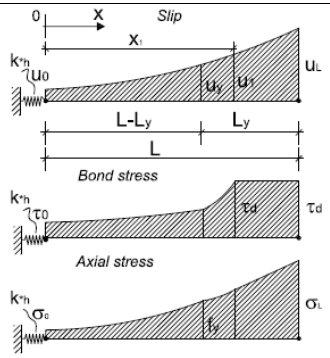		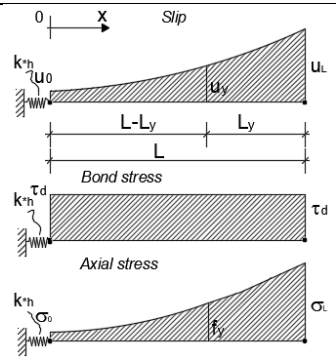	
$\sigma_L = \frac{4\cdot\tau_d\cdot L_y\cdot(u_L-u_y)+d_b\cdot f_y\cdot u_1\cdot\ln(\gamma_{Ly})}{d_b\cdot u_1\cdot\ln(\gamma_{Ly})}$ (21) $u_L = u_0 + \frac{\alpha_y\cdot[u_y-u_0(1+\ln(\gamma_{y0}))]}{[\ln(\gamma_{y0})]^2}$ $+\varepsilon_p\cdot L_y - \frac{f_y\cdot L_y}{E_h} +$ $-\frac{L_y\alpha_y}{(L-L_y)}\cdot\left\{\frac{L_y[-u_L+u_y\cdot(1+u_y\ln(\gamma_{Ly}))]}{\ln^2(\gamma_{Ly})}\right.$ (22) $\left.+\frac{(L-L_y)(u_0-u_y)}{\ln\gamma_{y0}}\right\}$ L_y is the length where the stress is higher than f_y: $L_y = L + \frac{d_b\cdot f_y\cdot u_1\cdot\ln(\gamma_{y0})}{4\cdot t_d\cdot(u_0-u_y)}$ (23)		$\sigma_L = \frac{4\tau_d L_y}{d_b} + f_y$ (24) $u_L = u_y + \frac{L_y}{d_b E_h}\cdot$ $\{d_b[E_h\varepsilon_p - f_y + k_h u_0] + 2\tau_d[2\cdot L - L_y]\} +$ (25) $-\frac{L_y}{d_b E_h}\left\{\frac{4\cdot(L-L_y)\cdot\tau_d[u_0+u_1\cdot(\ln(\gamma_{10})-1)]}{u_1\ln(\gamma_{y0})}\right\}$ L_y is given by (26) $L_y = \frac{4\tau_d L\vartheta + \rho u_1\ln(\gamma_{y0})}{4\cdot\tau_d\{u_0+u_1\cdot[\ln(\gamma_{1y})-1]\}}$ (26) $\rho = d_b\cdot(f_y - k_h u_0) - 4L\tau_d;$ $\theta = u_0 + u_1[(\ln(\gamma_{10})-1)]$ (27)		$\sigma_L = \frac{4\cdot L_y\cdot\tau_d\cdot[u_1(1-\ln(\gamma_{1L}))-u_y-1]+d_b\cdot f_y\cdot u_1\ln(\gamma_{Ly})}{d_b\cdot u_1\cdot\ln(\gamma_{Ly})}$ (28) $x_1 = \frac{\ln(\gamma_{1L})}{\ln(\gamma_{Ly})}\cdot L - L_y$ (29) $> L - L_y$ $L_y = L + \frac{d_b f_y u_1\cdot\ln(\gamma_{y0})}{4t_d(u_0-u_y)}$ (30) $u_L = u_0 + \Delta u_{L1} + \Delta u_{L2}$ (31) $\Delta u_{L1} = \frac{2E_s L_y^2\tau_d\gamma_{Y0}^2\{-2u_y(1+\gamma_{LY})+u_1[2(1+\gamma_{LY})+\gamma_{1L}^2]\}}{d_b E_h E_s u_1\gamma_{LY}^2\gamma_{Y0}^2}$ (32) $\Delta u_{L2} = \frac{\gamma_{LY}^2\cdot\{\upsilon + d_b\cdot E_s L_y u_1\gamma_{Y0}^2(E_h\cdot\varepsilon_p - f_y)\}}{d_b E_h E_s u_1\gamma_{LY}^2\cdot\gamma_{Y0}^2}$ (33) $\upsilon = -4\tau_d\cdot\Delta L_Y$ $\cdot[E_h\Delta L_Y(\Delta u_{0Y}+\gamma_{Y0}u_0)+\gamma_{Y0}E_s L_y\Delta u_{0Y}]$ (34) $\Delta L_Y = (L-L_y)$ $\Delta u_{0Y} = (u_0-u_y)$ (35)		$\tau(x) = \tau_d \quad 0 \le x \le L$ (36) $u_L = u_0 + \chi + \delta$ (37) $\sigma_L = k_h^*\cdot u_0 + \frac{4\tau_d}{d_b}L$ (38) $\chi = \frac{(L-L_y)\cdot(2L\tau_d - 2L_y\tau_d + d_b k_h u_0)}{d_b E_s}$ (39) $\delta = \frac{L_y[2\cdot(2L-L_y)\tau_d + d_b(E_h\varepsilon_p - f_y + k_h^* u_0]}{d_b E_h}$ (40) L_y is given by (41) $L_y = \frac{4L\tau_d + d_b k_h u_0 - d_b f_y}{4\tau_d}$ (41)	

Fig. 3 Analytical solution after yielding

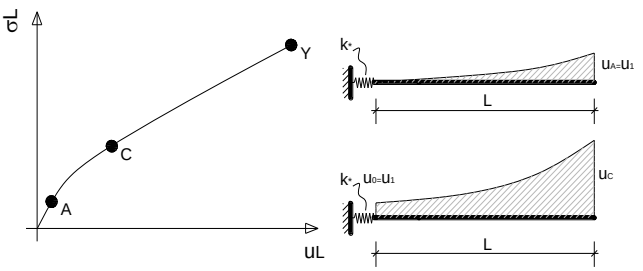

Fig. 4 Cardinal points for the new analytical formulation

steel, A_{gt} is the elongation to maximum load for the bar and ε_p is the deformation corresponding to the beginning of the hardening branch (i.e., end of the plateau).

$$E_h = \frac{f_u - f_y}{A_{gt} - \varepsilon_p} \tag{12}$$

In the following, the solutions in terms of stress and slip at the end of the bar, useful for the determination of the modified steel law to be assigned to rebars, are derived and presented. The analytical solution considers the different possible situations depending on the values of slip at the two ends, the different branches of the τ-u relationship and the slip values achieved at the ends, as well as already developed by Braga *et al*. (2012) and Braga *et al*. (2015).

These analytical solutions are reported, in terms of σ_L_u_L, before and after yielding in Figs. 2 and 3. The notation below has been followed.

4. Stress-slip law

The formulation showed in the previous paragraph provides a stress-slip (σ_L-u_L) relationship with three fundamental points corresponding to different physical status of the steel bar under relative slip. Points A, C, Y describe the behaviour of stress and slip in correspondence of the free end of the specimen embedded in the concrete block as simply presented in Fig. 4. In particular:

- *Point A*: represents the achievement of the limit bond stress τ_d at the free end of the bar: $u_{L,A}=u_1$.
- *Point C*: represents the point when all the length of the bar is characterized by a bond stress equal to τ_d. As a consequence $u_{0,C}=u_1$.
- *Point Y*: represents the achievement of yielding strength at the free end.

Figs. 5 (a)-(b) show the difference between the imposed and the deduced slip fields for the case $u_L \leq u_1$, $u_0 < u_1$ (bond stress lower than τ_d): as visible, the exponential model allows a good agreement of results is achieved.

The analytical stress-slip formulation (σ_L-u_L) provides the relationship between the stress and the relative slip at the end of the longitudinal bar: the application of the proposed model to nonlinear analysis with fiber elements, needs the transformation of the stress-slip relationship into a stress-strain one. In the case of fiber elements, the response is given by the weighted sum of individual representative sections whose position is selected by integration scheme. In particular, $L_i=w_p \cdot L$ is the portion of

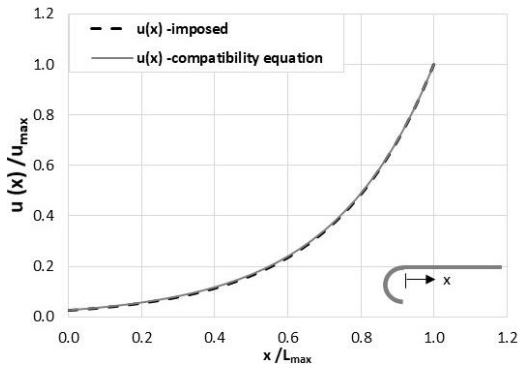

(a) exponential slip field (proposed model)

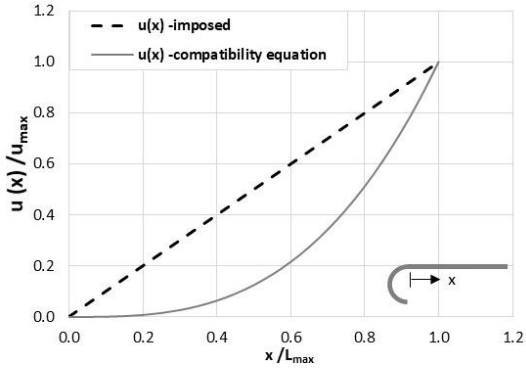

(b) linear slip field

Fig. 5 Imposed vs deducted slip field

element where the section response is assumed constant,being w_p the section weight.

The idea is to improve the (σ_L-u_L) in a fiber finite element as modified steel law, being u_L the integrated displacement of a longitudinal bar including both steel deformation and bond slip along the weighted length L_i of the elements ends, for a generic fiber. Consequently, Eq. (42) provides the transformation of displacement to pseudo-strain for a generic fiber, through the length of integration

$$\varepsilon^* = \frac{u_{L,TOT}}{L_i} \tag{42}$$

being ε* the 'pseudo-strain' including both bar's deformation and concrete-steel relative slip.

In Eq. (42) $u_{L,TOT}$ is the total relative displacement of the interested longitudinal bar, given by (43)

$$u_{L,TOT} = u_{L,A} + u_{L,B} \tag{43}$$

In which $u_{L,A}$ and $u_{L,B}$ are the relative displacements including the portion of slip regards to each block of concrete at the crack, as shown, for example, in Fig. 6.

The meaning of $u_{L,TOT}$ can be simply explained: the experimental flexural behaviour of RC elements (Gigliotti *et al*. 2002) is very similar to mechanisms of rigid bodies, with rotations concentrated in few sections, typically located at the ends of elements. The slip in correspondence of the crack opening represents the amplitude of the same crack ($u_{L,\ TOT}$), therefore allowing to determine the cyclic moment-curvature relationships of RC sections in fiber elements.

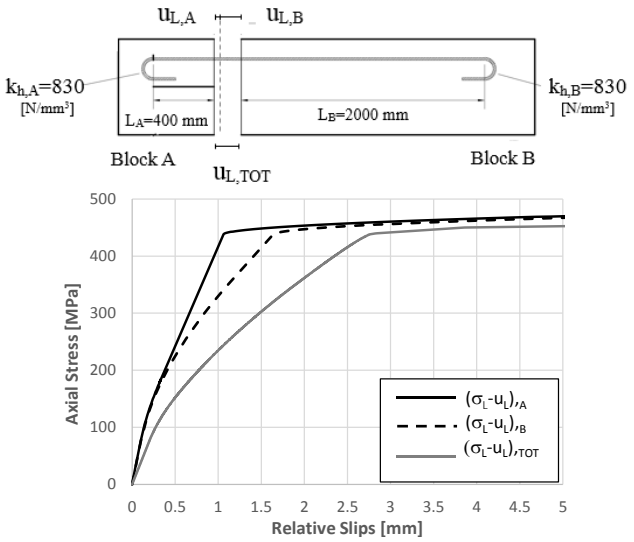

Fig. 6 Scheme of repartition of total slip within the crack

To obtain the modified steel law in terms of $(\sigma_L\text{-}u_L)_{TOT}$, is necessary to know $(\sigma_L\text{-}u_L)_{,A}$ and $(\sigma_L\text{-}u_L)_{,B}$ that depend on the characteristics of the two adjacent blocks and anchorages.

4.1 Influence of different parameters on the σ-u law

Fig. 7(a)-(d) highlight the differences in the stress-slip relationships obtained varying several parameters, i.e., diameter and length of the bar, bond strength and length of plateau. In particular, the diameter varies between 12 and 32 mm, the length of the bar between 600 and 6000 mm, the bond strength between 8 and 32 MPa and, finally, the length of the plateau depends on the strain at the end of it, ε_p, varying between 1% and 6%.

As visible, the increase of the bond strength gives lower slip for equal stresses, progressively approaching to the perfect bond conditions. On the other hand, the increase of diameter, length and yield plateau are related to higher values of relative slip.

5. Cyclic behavior

5.1 Numerical model and main assumptions

A parametric analysis was performed to achieve the formulation of the cyclic behaviour of the steel reinforcing bar including relative slip. The analyses were used to validate the shape and the behaviour of the monotonic branch, known from the analytical formulation, and to obtain the formulation of unloading and reloading branches related to the monotonic analytical formulation too.

The numerical model used for the parametric analysis was elaborated in OpenSees (Mazzoni *et al.* 2007), and consists in a steel bar modelled as truss element, bounded at one end with an elastic spring reproducing the hook, and N-links surrounding the bar introduced to simulate the bond slip behaviour (Fig. 8(a)). In the elaboration of the model, the following assumptions were made:

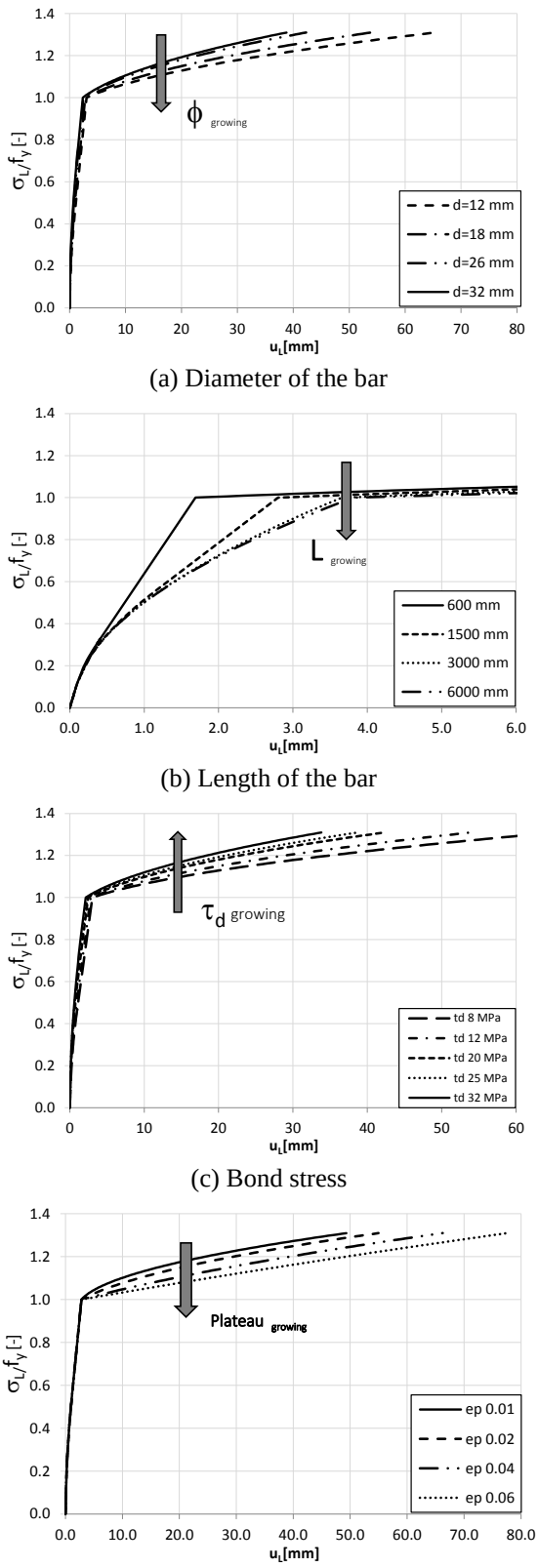

(a) Diameter of the bar

(b) Length of the bar

(c) Bond stress

(d) Length of the plateau

Fig. 7 Stress slip curves depending on different parameters

• The bar is provided by a typical steel behaviour including the hardening slope and the cyclic response following a modified Menegotto-Pinto law (Menegotto and Pinto 1973). The "Steel MPF" material (Filippou *et*

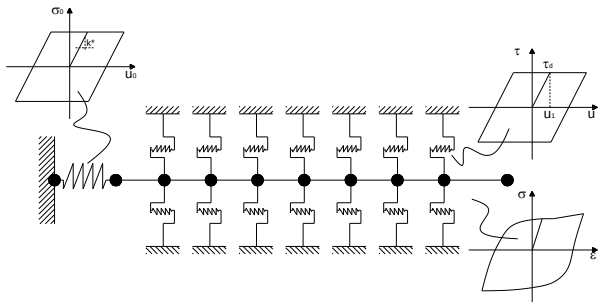

(a) Model

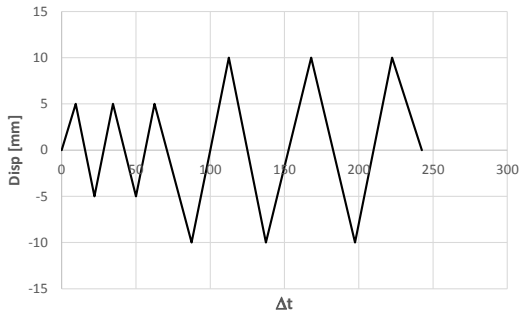

(b) Displacement history

Fig. 8 Numerical model for the cyclic behaviour of the steel bar subjects to slip

al. 1983), implemented in OpenSees, was used.

• An elastoplastic model, based on Model Code 1990 (CEB-FIP 1993), was adopted for the representation of the N-links simulating the bond-slip phenomena.

• The hook has an elastoplastic behaviour, according to the hypothesis of the analytical monotonic model.

The so modelled steel bar was subjected to increasing displacement histories imposed at the free end (Fig. 8(b)), according to different levels of ductility.

Parametrical analysis was then executed obtaining a regressive formulation, using parameters such as diameter and length of the bar, characteristics of the steel material (yield and maximum strength, plateau and maximum deformation), strength of concrete material, bond-slip law (using different bond strength τ_d and correspondent u_1).

Results allowed to connect the unloading and reloading curves to the monotonic analytical exponential formulation. To obtain an analytical formulation as close as possible to reality, the results coming from the experimental tests executed by Saatcioglu and Ozcebe (1989), Gigliotti *et al.* (2002) were taken into consideration.

5.1.1 Modelling of bond-slip relation for the N-links

Several analytical models describing the monotonic and cyclic problem of bond-slip for deformed bars were proposed in the current and past literature (e.g., Morita and Kaku 1973); however, no sufficient information is provided about plain bars, highly diffused in the case of existing buildings and whose performance strongly differ from the case of ribbed bars.

Abrams (1913), Verderame *et al.* (2009) executed several experimental test campaigns, analyzing both ribbed and plain bars, varying parameters such as diameter, embedded length, bar surface, concrete blocks dimensions,

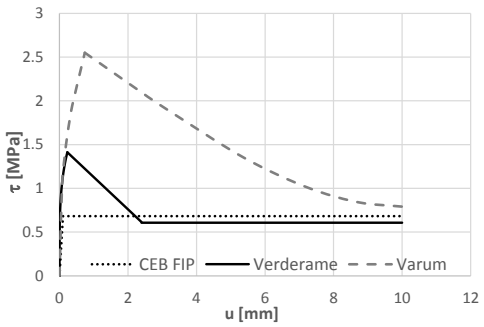

Fig. 9 Numerical examples using different models for bond slip monotonic law

Table 1 Relevant points for the description of the monotonic bond-slip relationship

Model adopted	$\tau_{b,\max}$ [MPa]	$\tau_{b,f}$ [MPa]	$s_{\max}$ [mm]	s_f [mm]
CEB-FIP	0.68	0.68	0.10	0.10
Verderame *et al.* (2004)	1.41	0.61	0.23	2.39
Varum	2.55	0.79	0.74	4.98

anchorage, storage conditions, age and concrete mix. Verderame *et al.* (2009) provided an analytical monotonic/ cyclic relationship for the stress-slip model for plain bars, described as function of the concrete strength. Melo *et al.* (2015) elaborated a very refined analytical monotonic model considering all the features influencing the bond-slip relationship, however with lack of details regarding the cyclic behaviour.

The bond-slip monotonic relationship generally shows three different branches: the first one describing the behaviour for very small slip (due to chemical adhesion, mechanical interaction between concrete and bar surface, friction, etc.) until the reaching of the peak strength; a second branch showing the effects of softening (different in the case of plain or deformed bars) due to the degradation of the friction resistance, and a third one governed by the residual friction strength.

Model Code (CEB-FIP 1993) provides an analytical model for the bond stress/slip law in which the ascending branch is described by a power function, extending the results provided by Eligehausen *et al.* (1983) for plain bars. The peak of the strength is neglected considering that it is lost after the first cycles. Verderame *et al.* (2009), Melo *et al.* (2015) proposed more detailed models based on the results of experimental tests, slightly different for the formulation of the softening branch.

The differences in the three considered monotonic models are presented in Fig. 9, while the values of significant points are presented in Table 1. As visible, the standard provisions can be considered conservative respect to experimental based models.

Concerning the cyclic behaviour, Model Code (CEB-FIP 1993) provides only the stiffness of the unloading branch with the average value equal to 200 N/mm^2. Verderame *et al.* (2009) determined the cyclic τ-u behaviour from experimental tests: the most interesting aspect of such experimentations consisted in the fact that in the reloading

branch of the cyclic behaviour the stresses did not reach the monotonic value of the friction strength but lower values, however not always simple to define.

Since the present work is mainly oriented to the determination of a model able to describe the cyclic/seismic behaviour of steel bars, the cyclic bond-slip relationship shall be defined.

Experimental tests previously mentioned, highlighted that the peak strength is lost immediately after first cycles due to friction and other phenomena: this focus the attention on the residual friction strength, remaining constant while relative slip increase. In the numerical analyses of the present work, the peak strength has been neglected, according to Model Code model (CEB-FIP 1993): for the cyclic behaviour of the N-link simulating the bond-slip, a simple elastoplastic law has been assumed.

5.1.2 Modelling of steel behavior

The behaviour of plain bars is different with the respect to the deformed bars too (Prota *et al*. 2009). Anyway, steel behaviour is characterized by many aspects, such as isotropic strain hardening, Baushinger effect with degradation in the loading and unloading cycles, yielding plateau, fatigue, buckling in compression etc., that need to be considered for the correct representation of the structural performance of RC sections and elements. However, the accuracy and the reliability of the numerical model shall be joined with the limitation, as much as possible, of the computational burden, to be applied also to the case of complex RC constructions.

In the present work, the *"SteelMPF"* model implemented in OpenSees (Mazzoni *et al*. 2007) was selected. The model follows the Menegotto-Pinto law with the addition of several features, such as the possibility to use different yield stress values and strain hardening ratios for tension and compression, the degradation of the cyclic curvature parameter R for strain reversals in both pre- and post-yielding regions etc. Fatigue and bucking phenomena were neglected, while kinematic strain hardening was included; the plateau was not modelled, since lost in the first few cycles, as visible from the execution of experimental tests (Caprili and Salvatore 2015).

Further numerical simulations were executed adopting the "Steel4" material model (Zsarnóczay and Budaházy 2013), more complicated from a computational point of view and then used only for a reduced number of analyses, to validate the adopted assumptions, finally providing positive results allowing to keep on with selected hypotheses.

5.2 Analytical formulation

Numerical parametrical analyses were executed with the aim of determining a cyclic formulation able to relate the unloading and reloading branch to the monotonic law, previously described. The shape of the unloading and reloading branches was defined in a normalized plane with to respect the yielding stress (f_y) and strain (ε_y) of each considered case: for example, Figs. 10(a)-(b) show different axial stress-slip curves obtained for several values of yielding strength. Adopting different values of bond

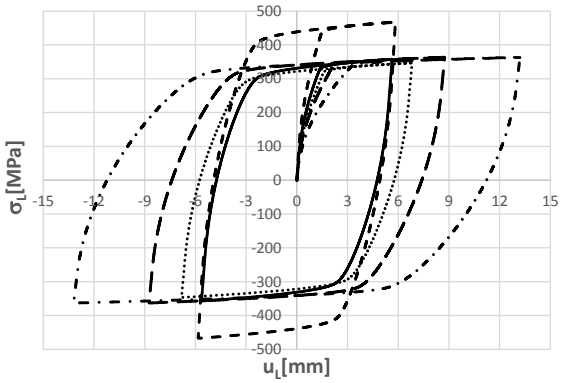

(a) Real

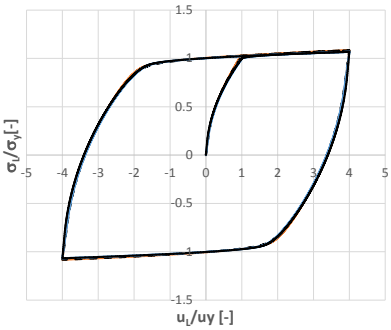

(b) Normalized

Fig. 10 Different σ-u plane with to respect to yielding point

strength, yield strength, length/diameters ratios, the results did not highlight significant variations of the cyclic shape of the curve.

In the loading branch, the cycles were characterized by 'cardinal point's, related to the ones identified in the monotonic formulation. Two main conditions can be observed:

- ***Case 1:*** point A, where the slip at the free end u_L is equal to u_1, and point Y, in which the stress at the free end σ_L is equal to σ_y.
- ***Case 2:*** point A, where the slip at the free end u_L is equal to u_1, point C where the anchorage slip u_0 is equal to u_1 (i.e., τ_d is constant along the bar) and point Y, in which the stress at the free end σ_L is equal to σ_y.

The first case is the most common, in which the anchorage length is lower than the total length of the bar and the bar yields before reaching the maximum bond strength for the entire length of the specimen. The second case concerns the situation in which both the length/diameter ratios and the strength are low (respectively of about 90 and 1.0 MPa).

The unloading branch is characterized by a first part (*SA'*) with stiffness equal to the elastic one of the first monotonic branch OA, so that K_A=$K_{SA'}$; the *SA'* branch is then followed by a descending curve until the reloading point *S'* is achieved.

From this point, a reloading branch (*S'A''*), characterized again by the same elastic stiffness of the first part, so that $K_{S'A''}$=$K_{A'}$ is defined and followed by the reloading curve (Figs. 11(a)-(b)).

The curvatures of the unloading and reloading curves are defined in function of the deterioration parameters of

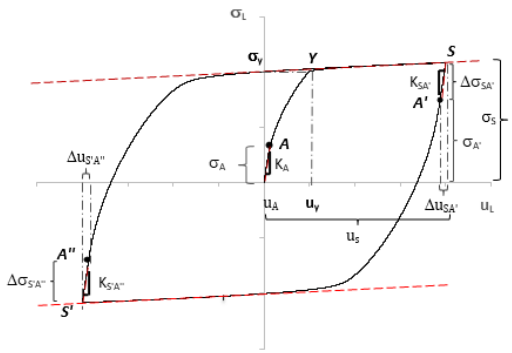

(a) Real

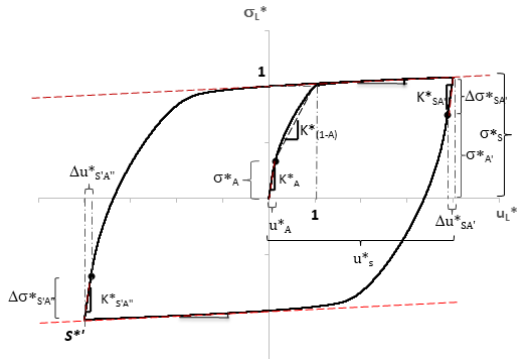

(b) Normalized

Fig. 11 Cardinal cyclic points in different *σ-u* plane with to respect to yielding point

Menegotto-Pinto law, while the subsequent cycles follow the typical trend of kinematic hardening (Fig. 11). The regressions on numerical curves allow obtaining the following expressions for the unloading and reloading curves in the normalized plane (Eq. (44))

$$\sigma^* = a \cdot \left[\frac{(u^* - u_S^*)}{b} \right]^n + \sigma_S^* \tag{44}$$

Where σ^* and u^* represent, respectively, the normalized stress and slip and a and b are defined according to Eqs. (45)-(48)

$$\sigma^*_i = \frac{\sigma_i}{\sigma_Y} \tag{45}$$

$$u^*_i = \frac{u_i}{u_Y} \tag{46}$$

$$a = (\sigma^*_{A'} - \sigma^*_S) \tag{47}$$

$$b = (u^*_{A'} - u^*_S) \tag{48}$$

The coordinates of point S can be found by Eqs. (49)-(50) considering the following expressions where represents the level of ductility.

$$u_s = \mu \cdot u_y \tag{49}$$

$$\sigma_s = \frac{(u_s - u_y)}{(u_u - u_y)} \cdot (\sigma_u - \sigma_y) + \sigma_y \tag{50}$$

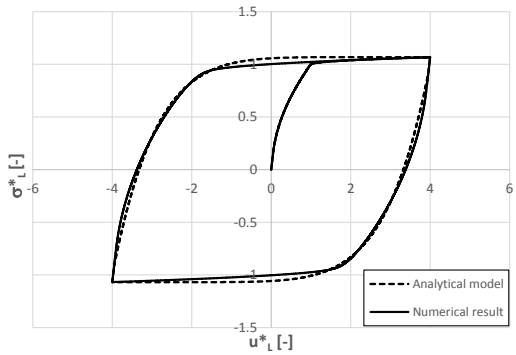

Fig. 12 Comparison between numerical model and analytical proposed model

To describe the unloading and reloading curves is necessary to define the coordinates of points *A'* (u_A' and σ_A') and of *A''* (u_A'' and σ_A''), that can be derived as a function of the coordinates of point *A*, defined in the monotonic branch (Eqs. (51) -(52))

$$u_A' = \left(u_S^* - \Delta u_{SA'}^*\right) \cdot u_y \tag{51}$$

$$\sigma_A' = \left(\sigma_S^* - \Delta\sigma_{SA'}^*\right) \cdot \sigma_y \tag{52}$$

Being

$$\Delta\sigma_{SA'}^* = \sigma_A^* \tag{53}$$

$$\Delta u_{SA'}^* = u_A^* \tag{54}$$

Eq. (55) shows the trend of the stiffness in the branch (*SA'*)

$$K_{SA'}^* = K_A^* \tag{55}$$

The value of the exponent n of Eq. (44) is given by the followings Eqs. (56)-(57), respectively for Case 1 and 2.

$$n = 1.82 \cdot \mu + 0.29 \tag{56}$$

$$n = 1.56 \cdot \mu + 0.09 \tag{57}$$

Being μ the ductility and is expressed by u_{max}/u_Y.

Eqs. (56)-(57) expresses the exponent n of the unloading and reloading branch only in function of the ductility μ. The dependence of the parameter n from different features such as yield stress, bond strength, length/diameter ratio, for different level of ductility, is, in fact, not relevant.

It is then clear that the shape of the cycles (depending on parameter n) does not change significantly with different bar parameters, essentially depending only from the ductility. Fig. 12 shows the good agreement between numerical and the proposed analytical model.

6. Validation of the proposed cyclic model

6.1 Saatcioglu and Ozcebe (1989), Specimen "U4"

To validate the analytical model, the experimental test "U4" by Saatcioglu and Ozcebe (1989), was reproduced.

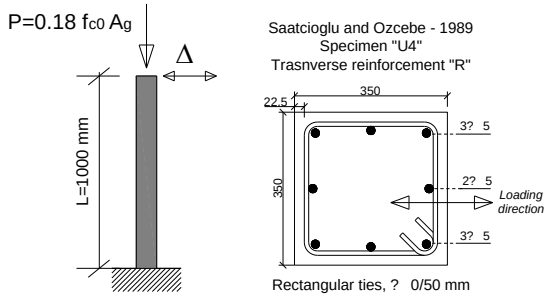

(a) Section geometry

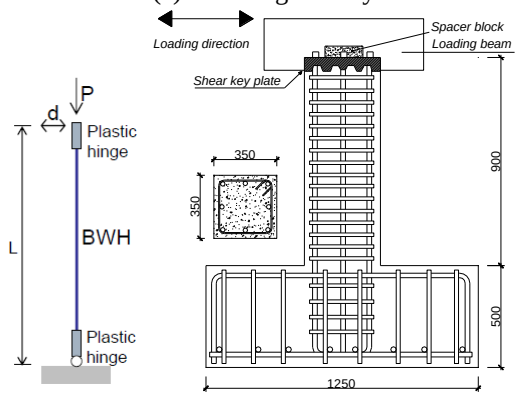

(b) Schematization of real model

Fig. 13 Saatcioglu and Ozcebe (1989) specimen U4

The case study consists in a cantilever beam subjected to a lateral top displacement with a constant axial load equal to 600 kN and square section with a typical flexural collapse. The yield strength of steel bars was equal to 438 MPa, the bond strength was equal to 2.0 MPa and u_1 was equal to 0.1 mm. Figs. 13(a)-(b) show the geometry, details and load application to the test specimen.

The cantilever beam was modelled in OpenSees (Mazzoni *et al*. 2007), using Beam With Hinges element, characterized by two plastic hinges of specified length in correspondence of the two ends and one elastic central part.

The stress-slip law must be shifted in a stress-strain law, using an opportune hinge length L_p, that - in the present case - was formulated according to Paulay and Priestley (1992). The total slip was provided by the sum of slip near to opening crack: the first slip is related to the portion of concrete block in hook region, called L_A, representing the slip of the bar respect to the concrete block, while the second slip is related to the straight bar, called L_B, representing the slip of the concrete respect to the bar. Obviously, the slip related to concrete block in the hook region has a lower value than the on provided by the straight bar, so that the total σ-u is given by the contribution of two laws (Figs. 14(a)-(b)).

For the modelling of the concrete, the BGL model (Braga *et al*. 2006) was assumed; for reinforcing steel bars the analytical model previously elaborated and described was adopted.

The comparison between the experimental and the numerical results are presented in Fig. 15. Results of numerical analyses confirmed that the hypothesis of perfect bond is not sufficient to reproduce the actual response of the

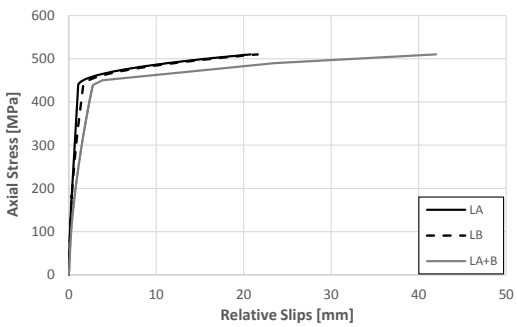

(a) σ-u model

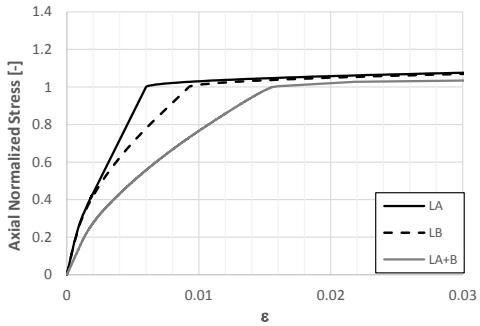

(b) σ-ε relation

Fig. 14 Relationship referred to two blocks

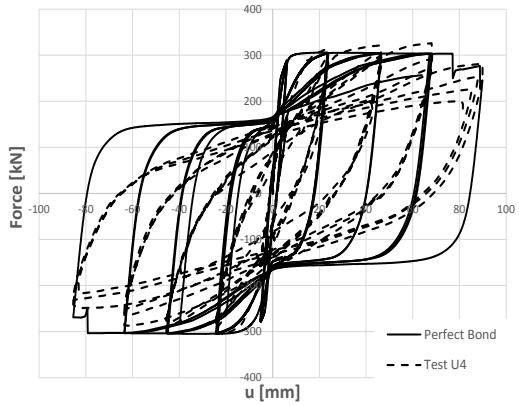

(a) Perfect bond

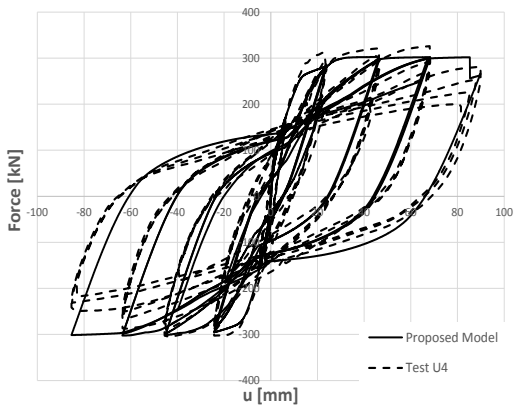

(b) Bond slip

Fig. 15 Experimental vs Numerical results

structural RC element; the overestimation of the energy dissipation is highlighted: perfect bond condition

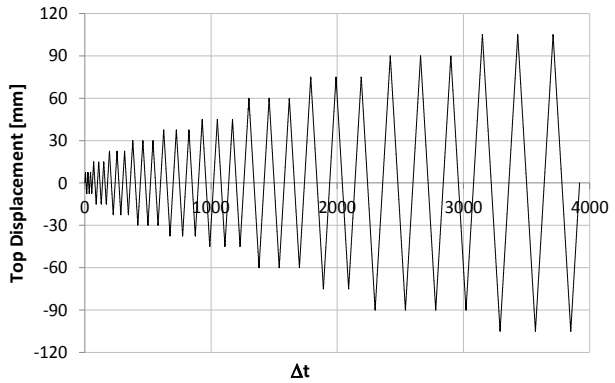

Fig. 16 Displacement history applied at the top of the column

overestimates of 30% the energy dissipated in the actual response, such as the initial stiffness. On the contrary, the modelling of bond-slip allows to capture the actual response, in terms abovementioned.

6.2 Braga, Gigliotti, Laterza (2002)

The case study consists in a beam-column joint designed only for vertical loads and with plain bars. At the top of the upper column, a constant axial load of 270 kN was applied and the specimen was subject to cyclic load reversal. The beam-column joint was modelled in OpenSees (Mazzoni *et al*. 2007) using BeamWithHinges elements. Materials presented the following properties: concrete compressive strength (f_{cm}) 22.47 MPa, steel yielding strength (f_y) 340 MPa, steel tensile strength (f_u) 430 MPa, steel maximum deformation 30%. Following the value of concrete strength f_{cm}, according to Model Code (CEB-FIP 1993), the value of bond strength τ_d was assumed equal to 0,7 MPa, u_1 equal to 0.1 mm and hook stiffness k_h* equal to 670 N/mm^3.

The top of the column was subject to a horizontal displacement history as presented in Fig. 16. Figs. 17(a)-(d) present the general geometry of the interior joint, while Figs. 18(a)-(f) and Figs. 19(a)-(b) show the constitutive laws used for concrete and bars. More information about the tests are provided in Gigliotti *et al*. (2002).

The stress-slip law was shifted to a stress-strain law, through hinge length L_p equal to $H/3$ (where H is the high of section), according to the experimental test results. The stress- pseudo strain laws are also shown in Fig. 18, while, as an example, in Fig. 19(b) are presented the differences between the same laws in case of bond slip hypothesis and perfect bond, for column's bars.

The results of numerical analyses in terms of horizontal column force vs. top displacement (Figs. 20(a)-(b)) confirmed that the perfect bond hypothesis is not sufficient to describe the real behaviour of the beam-to-column joint. In particular, perfect bond gives an initial stiffness that is twice the real stiffness and overestimates it in the last cycles until four times. The perfect bond overestimates, furthermore, the dissipated energy for each cycle, while bond slip hypothesis gives a reasonable indication according with the experimental results.

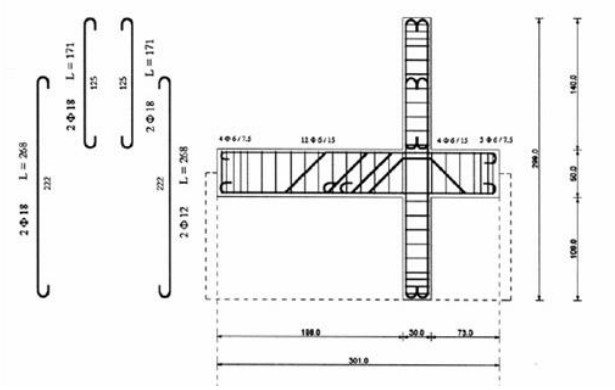

(a) Column bars

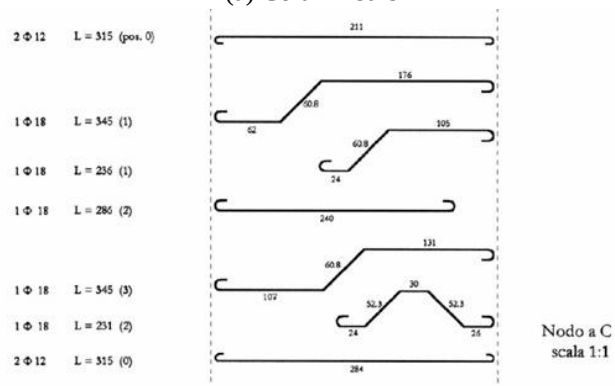

(b) Beam bars

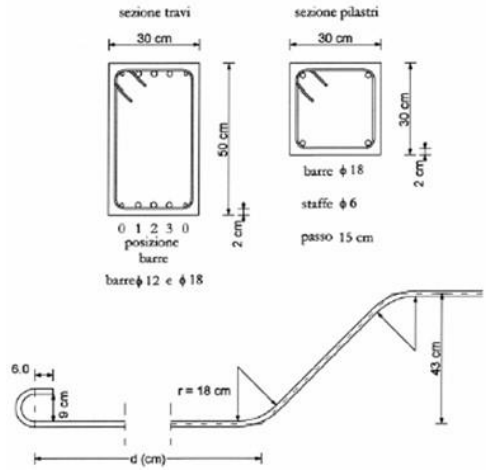

(c) Section details

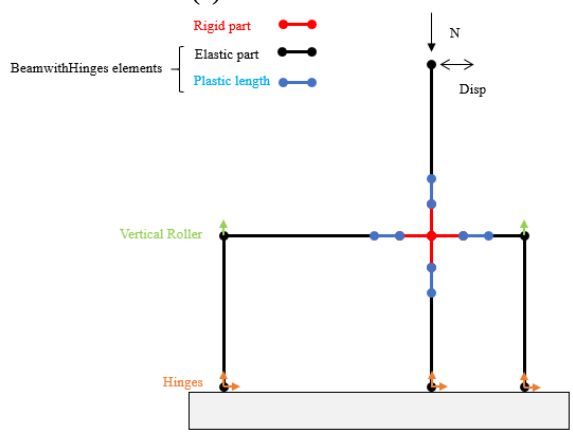

(d) Scheme of numerical model

Fig. 17 Interior beam column joint

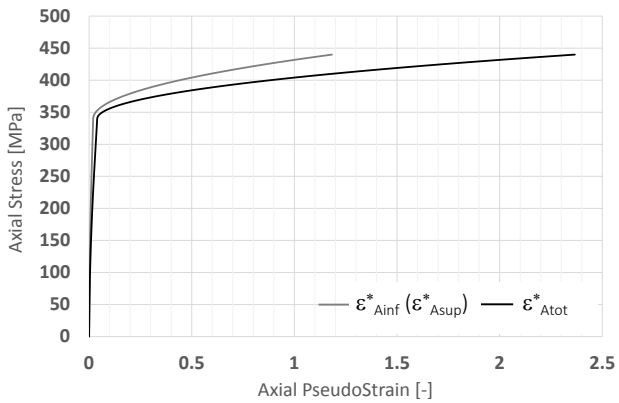

(a) Column monotonic

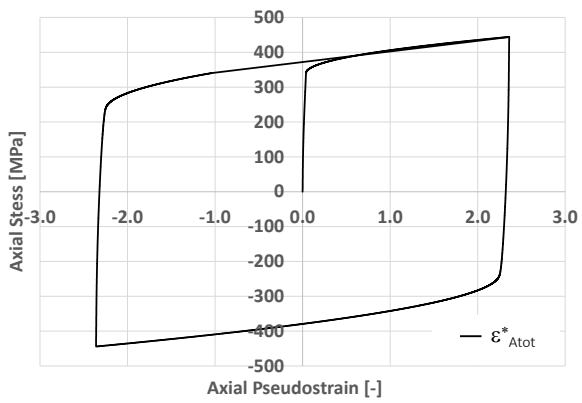

(b) Column cyclic

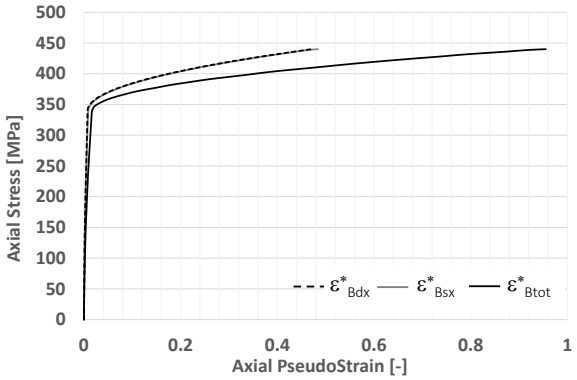

(c) Beam *d* 12 monotonic

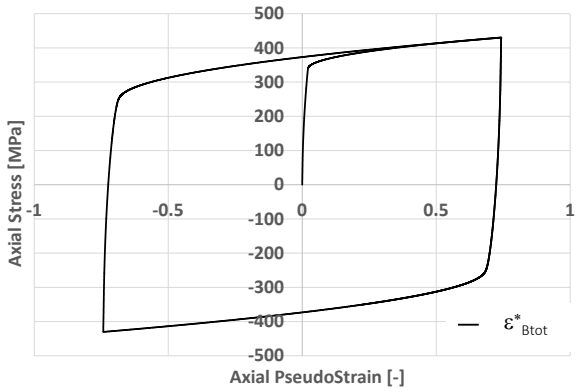

(d) Beam *d* 12 cyclic

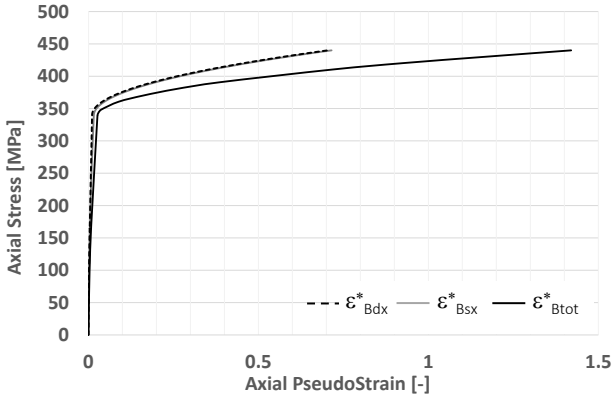

(e) Beam *d* 18 monotonic

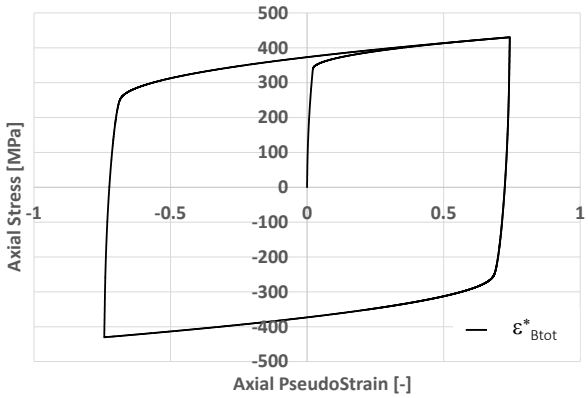

(f) Beam *d* 18 cyclic

Fig. 18 Modified monotonic and cyclic steel law for different bars

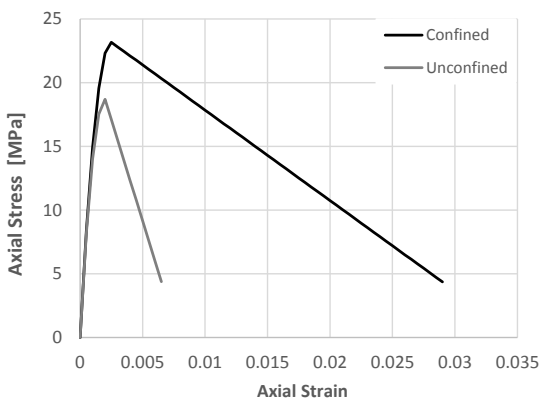

(a) σ-ε concrete

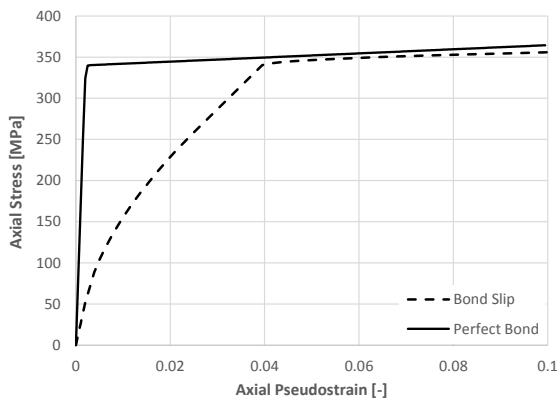

(b) σ-ε bars (Bond Slip vs Perfect Bond)

Fig. 19 Materials constitutive laws

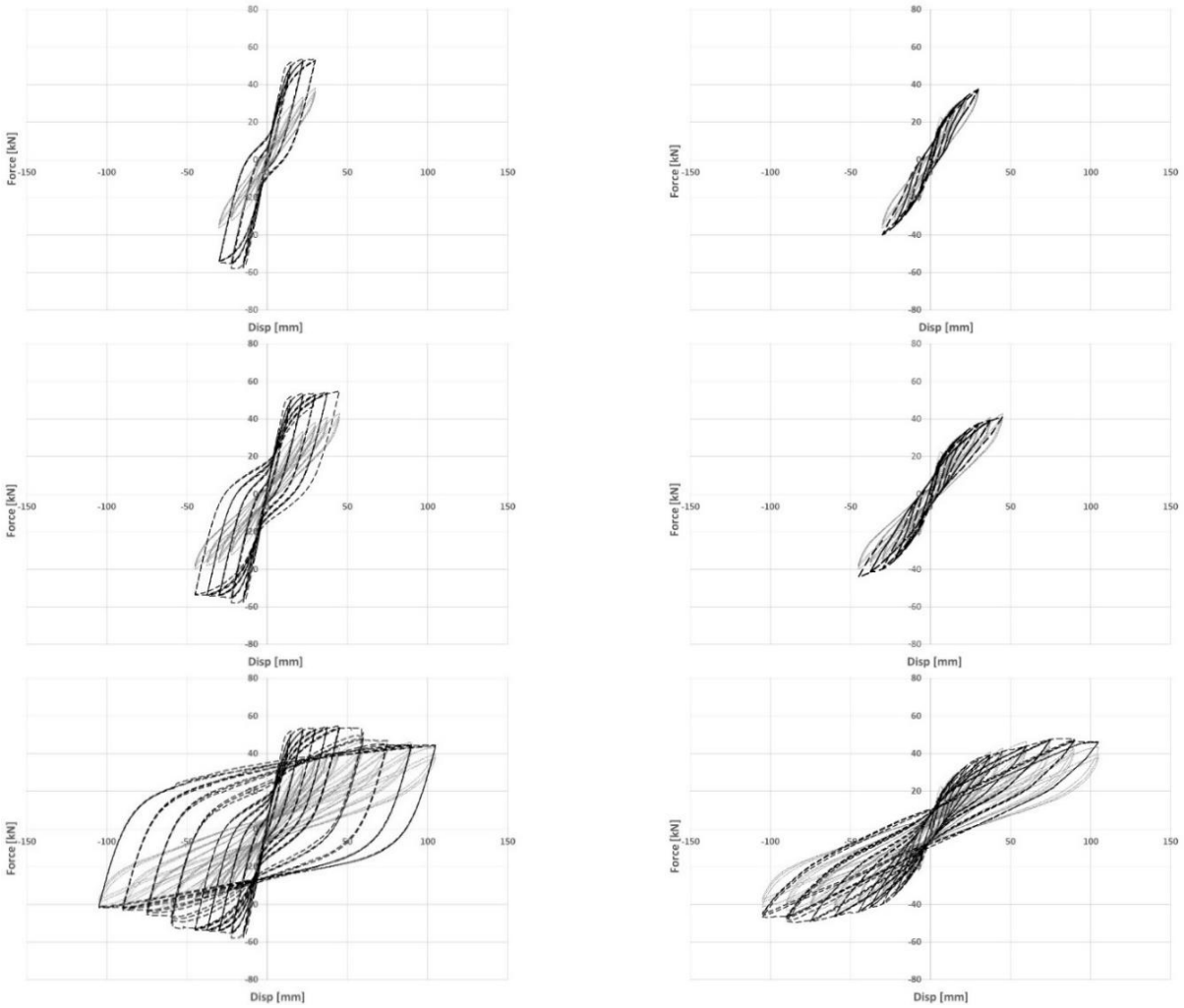

(a) Full bond (b) Bond slip

Fig. 20 Beam column joint response: horizontal column force-top displacement

7. Conclusions

A new simplified exponential cyclic formulation is proposed to describe modified the constitutive stress-strain law of steel reinforcing bars, directly including relative slip between bars and surrounding concrete. The proposed model aims to complete and deepen the original Braga *et al.* (2012) model, being able to overcome its inconsistencies regarding the cubic deduced slip, including hardening but simplifying the analytical formulation provided by Braga *et al.* (2015) and, mostly, to provide an analytical description of cyclic behaviour through the description of unloading and reloading branches. The cyclic proposed formulation, for its simplicity, can be used for the nonlinear analysis of RC structures, especially when plain bars are used: in this case the issue of relative slip between bars and concrete is, in fact, very important, while neglecting it often leads to wrong prediction of the structural response.

Validations of the proposed model with experimental results have been executed, highlighting the adequacy of the model to estimate the actual structural response, in particular compared to the perfect bond hypothesis.

References

Abrams, D.A. (1913), “Tests of bond between concrete and steel”, Engineering Experiment Station, University of Illinois at Urbana Champaign, College of Engineering, Champaign, IL, USA.

Apostolopoulos, C., Ascanio, C., Bianco, L., Braconi, A., Caprili, S., Diamantogiannis, G., Ferreira Pimenta, G., Finetto, M., Moersch, J. and Salvatore, W. (2014), “Effects of corrosion on low-cycle fatigue (seismic) behaviour of high strength steel reinforcing bars”, RFSR-CT-2009-00023 Project, Final Report, European Commission, Brussels, Belgium.

Braconi, A., Braga, F., Caprili, S., Gigliotti, R. and Salvatore, W. (2014), “Seismic demand on steel reinforcing bars in reinforced concrete frame structures”, *Bull. Earthq. Eng.*, **12**(6), 2633-2664.

Braga, F., Caprili, S., Gigliotti, R. and Salvatore, W. (2015), “Hardening slip model for reinforcing steel bars”, *Earthq. Struct.*, **9**(3), 503-539.

Braga, F., Gigliotti, R. and Laterza, M. (2006), “Analytical stress-strain relationship for concrete confined by steel stirrups and/or FRP jackets”, *J. Struct. Eng.*, **132**(9), 402-1416.

Braga, F., Gigliotti, R. and Laterza, M. (2009), “R/C existing structures with smooth reinforcing bars: experimental behaviour of beam-column joints subject to cyclic lateral loads”, *Open*

Constr. Build. Technol. J., **3**, 52-67.

Braga, F., Gigliotti, R., Laterza, M., D'Amato, M. and Kunnath, S. (2012), "Modified steel bar model incorporating bond-slip for seismic assessment of concrete structures", *J. Struct. Eng.*, **138**(11), 1342-1350.

Caprili, S. and Salvatore, W. (2015), "Cyclic behaviour of uncorroded and corroded steel reinforcing bars", *Constr. Build. Mater.*, **76** ,168-186.

Caprili, S., Moersch, J. and Salvatore, W. (2015), "Mechanical performance vs. corrosion damage indicators for corroded steel reinforcing bars", *Adv. Mater. Sci. Eng.*, **2015**, Article ID 739625, 19.

CEB-FIP Model Code 1990 Design Code (1993), Comitè Euro-International du Beton.

D'Amato, M., Braga, F., Gigliotti, R., Kunnath, S. and Laterza, M. (2012), "Validation of a modified steel bar model incorporating bond slip for seismic assessment of concrete structures", *J. Struct. Eng.*, **138**(11), 1351-1360.

Dehestani, M. and Mousavi, S.S. (2015), "Modified steel bar model incorporating bond-slip effects for embedded element method", *Constr. Build. Mater.*, **81**, 284-290.

Eligehausen, R., Popov, E.P. and Bertero, V.V. (1982), "Local bond stress-slip relationships of deformed bars under generalized excitations", *7th European Conference on Earthquake Engineering*, Athens, Greece.

Fernandes, C., Varum, H. and Costa, A. (2013), "Importance of the bond-slip mechanism in the numerical simulation of the cyclic response of RC elements with plain reinforcing bars", *Eng. Struct.*, **56**, 396-406.

Filippou, F.C., Popov, E.P. and Bertero, V.V. (1983), "Effects of bond deterioration on hysteretic behaviour of reinforced concrete joints", Earthquake Engineering Research Center, Report UCB/EERC-83/19, Univ. of Calif., Berkeley.

Gigliotti, R. (2002), "Strutture in C.A. progettate per soli carichi verticali: sperimentazioni su nodi trave-pilastro", Ph.D. Dissertation, University of Salerno and University of Basilicata, Italy.

Hakuto, S., Park, R. and Tanaka, H. (2000), "Seismic load tests on interior and exterior beam-column joints with substandard reinforcing details", *ACI Struct. J.*, **97**(1), 11-25.

Kwak, H.G. and Filippou, F.C. (1995), "A new reinforcing steel model with bond-slip", *Struct. Eng. Mech.*, **3**(4), 299-312.

Laterza, M., D'Amato, M. and Gigliotti, R. (2017), "Modeling of gravity-designed RC sub-assemblages subjected to lateral loads", *Eng. Struct.*, **130**, 242-260.

Lowes, L. and Altoontash, A. (2003), "Modeling reinforced-concrete beam-column joints subjected to cyclic loading", *J. Struct. Eng.*, **129**(12), 1686-1697.

Lowes, L.N. (1999). "Finite element modeling of reinforced concrete beam-column bridge connections", Ph.D Dissertation, University of California, Berkeley.

Mazzoni, S., McKenna, F., Scott, M.H., Fenves, G.L. and Jeremic, B. (2007), *Opensees Command Language Manual*, Pacific Earthquake Engineering Research (PEER) Center.

Melo, J., Rossetto, T. and Varum, H. (2015), "Experimental study of bond-slip in RC structural elements with plain bars", *Mater. Struct.*, **48**(8), 2367-2381.

Melo, J., Varum, H. and Rossetto, T. (2015), "Cyclic behaviour of interior beam-column joints reinforced with plain bars", *Earthq. Eng. Struct. Dyn.*, **44**(9), 1351-1371.

Menegotto, M. and Pinto, P.E. (1973), "Method of analysis for cyclically loaded RC plane frames including changes in geometry and non-elastic behavior of elements under combined normal force and bending" , *IABSE Symposium on Resistance and Ultimate Deformability of Structures Acted on by Well-Defined Repeated Loads*, Lisbon, Portugal.

Mitra, N. and Lowes L. (2007), "Evaluation, calibration, and verification of a reinforced concrete beam-column joint model", *J. Struct. Eng.*, **133**(1), 105-120.

Mohammad, A.F., Faggella, M., Gigliotti, R. and Spacone, E. (2014), "Influence of bond-slip effect and shear deficient column in the seismic assessment of older infilled frame R/C structures", *Proceedings of EURODYN 2014 9th International Conference on Structural Dynamics*, Porto, June.

Monti, G. and Spacone, E. (2000), "Reinforced concrete fiber beam element with bond-slip", *J. Struct. Eng.*, **126**(6), 654-661.

Monti, G., Filippou, F.C. and Spacone, E. (1997), "Analysis of hysteretic behavior of anchored reinforcing bars", *ACI Struct. J.*, **123**(5), 248-260.

Morelli, F., Amico, C., Salvatore, W., Squeglia, N. and Stacul, S. (2017), "Influence of tension stiffening on the flexural stiffness of reinforced concrete circular sections", *Mater.*, **10**(6), 669.

Morita, S. and Kaku, T. (1973), "Local bond stress-slip relationship under repeated loading", *IABSE Symposium*, Lisbon, Portugal

Pauley, T. and Priestley, M.J.N. (1992), *Seismic Design of Reinforced Concrete and Masonry Buildings*, John Wiley and Sons, New York, NY, USA.

Prota, A., De Cicco, F. and Cosenza, E. (2009), "Cyclic behavior of smooth steel reinforcing bars: Experimental analysis and modeling issues", *J. Earthq. Eng.*, **13**(4), 500-519.

Saatcioglu, M. and Ozcebe, G. (1989), "Response of reinforced concrete columns to simulated seismic loading", *ACI Struct. J.*, **86**(1), 3-12.

Sezen, H. and Setzler, E.J. (2008), "Reinforcement slip in reinforced concrete columns", *ACI Struct. J.*, **105**(3), 280-289

Verderame, G.M., De Carlo, G., Ricci, P. and Fabbrocino, G. (2009), "Cyclic bond behaviour of plain bars. Part II: Analytical investigation", *Constr. Build. Mater.*, **23**(12), 3512-3522.

Verderame, G.M., Ricci, P., De Carlo, G. and Manfredi, G. (2009), "Cyclic bond behaviour of plain bars. Part I: Experimental investigation", *Constr. Build. Mater.*, **23**(12), 3499-3511.

Zsarnóczay, Á. and Budaházy, V. (2013), "Uniaxial material model development for nonlinear response history analysis of steel frames", *Proceedings of 2nd Conference of Junior Researchers in Civil Engineering*, June.

AT

Notations

Symbol	Description
d_b	longitudinal bar diameter
A_b	cross section of the bar
L	bar embedment length
L_0	anchorage length
R	hook radius
E_s	elastic steel modulus
E_h	secant steel modulus of the hardening branch
s	abscissa along the hooked end
x	abscissa along the straight bar
σ	stress along the embedded bar
τ_d	bond strength
u_L	slip at the free end of embedded bar
u_0	slip at the embedded end
u_1	slip where d is attained
x_1	abscissa along the bar in which = d
ε_y	steel yield strain
ε_p	steel strain at the end of plateau;

ε^*	pseudo-strain along the embedded bar
A_{gt}	steel deformation at the maximum stress
L_y	length of embedded bar yielded
k_h*	normalized stiffness of the linear spring (hook)